Available online at www.sciencedirect.com
SCIENCE DIRECT®
Journal of Magnetic Resonance 172 (2005) 31–35
JMR Journal of Magnetic Resonance
www.elsevier.com/locate/jmr

Communication

An NMR technique for rapid measurement of flow

Yi-Qiao Song*, Ulrich M. Scheven

Schlumberger-Doll Research, 36 Old Quarry Road, Ridgefield, CT 06877, United States

Received 20 June 2004; revised 8 September 2004

Abstract

We present a one-scan method for determining fluid flow velocity within a few milliseconds in the presence of a static field gradient, and without the need of multiple scans. A few RF-pulses populate a series of coherence pathways, each of which exhibits a phase shift that is proportional to fluid velocity. These coherence pathways produce spin echoes separated in the time domain, thus eliminating the need for phase cycling.

Keywords: Coherence pathways; Field gradient; Flow-induced phase shift; One-scan method

1. Introduction

NMR flow measurements are useful in studying natural or industrial processes, and in fluid characterization. The measurements employ static or pulsed magnetic field gradients. The essential idea of the pulse sequences, based on the work of Hahn [1] and Stejskal and Tanner [2], is to first use a static or pulsed field gradient to create a sinusoidal spatial modulation of spin magnetization, characterized by a magnetic wave vector k, which is proportional to encoding time and gradient strength. After some evolution time the displacement of spins by the flow field causes a phase shift of the modulation, which is evident in the NMR signal. The phase shift is proportional to the linear velocity and the wave vector k, for symmetric displacement distributions. With the standard methods, the measurement of flow velocity [3] requires a separate scan for each chosen modulation k, and generally phase cycling is further needed to select the desired coherence pathway.

This paper introduces a method to measure flow that uses a single scan acquisition to acquire data at a series of modulations, without a need for phase cycling.

* Corresponding author. Fax: +1 203 438 3819.
E-mail address: ysong@slb.com (Y.-Q. Song).

1090-7807/$ - see front matter © 2004 Elsevier Inc. All rights reserved.
doi:10.1016/j.jmr.2004.09.018

2. Theory

2.1. Spatial modulation of spin magnetization

In the presence of a magnetic field gradient $\mathbf{g}$, the transverse magnetization precesses to accumulate a phase ϕ. The rate of the phase accumulation is proportional to the local magnetic field, $B(\mathbf{x}) = B_0 + \mathbf{g}\cdot\mathbf{x}$, where $\mathbf{x}$ is a position vector

$$\frac{\mathrm{d}\phi}{\mathrm{d}t} = q\gamma[\mathbf{g}\cdot\mathbf{x} + B_0], \tag{1}$$

where q is the magnetization state, $q = 1$ for M_+, $q = -1$ for M_- and $q = 0$ for M_0. We shall ignore the constant term since it is the same for the entire sample. For molecules moving at a constant velocity $\mathbf{v}$, the above equation can be rewritten in the integral form:

$$\phi(\mathbf{x}_0) = \int_0^T q(t)\gamma\mathbf{g}\cdot(\mathbf{v}t + \mathbf{x}_0)\,\mathrm{d}t, \tag{2}$$

$$= \phi_1 + \phi_0. \tag{3}$$

Here T is the echo time and the position of the spin is linear in time, $\mathbf{x} = \mathbf{v}\cdot t + \mathbf{x}_0$. $\mathbf{x}_0$ is the initial position at time zero and is distributed within the entire sensitive region of the sample.

Notice that there are two terms contributing to the phase. The first term is the same for the entire sample and it is a function of **v**:

$$\phi_1 = \int_0^T q(t)\gamma \mathbf{g}\cdot \mathbf{v}t\,\mathrm{d}t, \tag{4}$$

$$= \gamma v \int_0^T q(t) g_v(t) t\,\mathrm{d}t, \tag{5}$$

$$= v \cdot c_Q. \tag{6}$$

Here, v is the magnitude of the velocity and g_v is the gradient along the velocity. Note that the time dependence of the gradient is explicit in Eq. (5). We introduce the coefficient c_Q to denote the sensitivity of the coherence pathway (Q) to the velocity

$$c_Q \equiv \gamma \int_0^T q(t) g_v(t) t\,\mathrm{d}t. \tag{7}$$

The second term, $\phi_0 = \gamma \mathbf{x}_0 \cdot \int_0^T \mathbf{g} q(t)\,\mathrm{d}t$, does not depend on **v**, but it is spatially dependent. This phase factor often causes the FID signal to decay rapidly and is the basis for MRI. An echo will form when ϕ_0 becomes zero for all positions and the residue phase of the echo (ϕ_1) will be proportional to the velocity.

2.2. Multiple modulation multiple echoes (MMME)

Consider a static magnetic field gradient, a train of three pulses with tipping angles α_1, α_2, and α_3, and the time spacing between them to be τ_1, τ_2,

$$\alpha_1 - \tau_1 - \alpha_2 - \tau_2 - \alpha_3 - \text{acquisition}. \tag{8}$$

The nutation angles of the pulses are *not* necessarily multiples of 90°. In the presence of constant field gradients, for instance, the nutation angle of a pulse will depend on the frequency offset and may not be the same for the entire sample. Typically, we use $\tau_2 = 3\tau_1 \equiv 3\tau$, and the motivation for it will be explained later. Usually, the above sequence will allow a total of five coherence pathways to produce five signals

echo time	q_1	q_2	$\phi_1/(\gamma g v \tau^2)$
0	0	0	0
τ_1	1	0	−4
$\tau_2 - \tau_1$	−1	1	−3
τ_2	0	1	−9
$\tau_2 + \tau_1$	1	1	−16

(9)

Here, the velocity-dependent phase, ϕ_1, is listed for each coherent pathway. q_1 and q_2 are the magnetization states during τ_1 and τ_2. Each coherence pathway is characterized by four numbers, $Q = (q_0, q_1, q_2, q_3)$ with $q_0 = 0$ and $q_3 = -1$. The formalism using these Q's to understand diffusion has been recently discussed in [4,5].

During the periods of τ_1 and τ_2, transverse magnetization ($q = \pm 1$) will acquire a phase of $\gamma g x q_i \tau_i$ ($i = 1$ and 2), thus the echo appears when the phase factor ϕ_0 is zero for the entire sample

$$q_1\tau_1 + q_2\tau_2 - \tau_3 = 0, \tag{10}$$

where τ_3 is the time after the last pulse for the echo to appear, thus $\tau_3 \geqslant 0$. When the ratio of τ_1 and τ_2 is set to 1:3, all echoes are separated by τ_1.

Different coherence pathways create different spatial phase modulation and they yield echo signals at different times, completely separable. As a result, in one scan of the sequence, five different modulations or echoes can be measured and five flow-induced phases (ϕ_1) can be determined. From these ϕ_1's, flow velocity can be determined easily.

The extension of this 3-pulse sequence to one with N pulses has been discussed in details for the measurement of diffusion [6]. This class of sequences is called multiple modulation multiple echoes (MMME). For example, with four pulses (MMME4), 13 echoes can be recorded, providing 13 different modulations. In general, for N pulses, a total of

$$\frac{3^{(N-1)} - 1}{2} + 1$$

signals of different c_Q can be obtained. This is one of the unique advantages of the MMME technique that the number of modulations is exponential with respect to the number (N) of RF pulses. To separate all echo signals in the acquisition time domain, the adjacent time periods (τ_i and τ_j) should follow the ratio of 3, for example,

$$\tau_{i+1} = 3 \cdot \tau_i. \tag{11}$$

Also, the pulses are not limited to small tipping angles, in contrast to several previously reported fast methods, e.g., [7–9].

Although these previous fast methods [7–9] were intended primarily for diffusion measurement, they are equally sensitive to coherent flow and the phase change of the echoes can be used as a measure of flow. These methods produce multiple modulations by applying a series of small tipping angle pulses (often less than 1°) and multiple echoes are to be detected in a fashion similar to spin-echo [7,9] and stimulated echo [8]. In these schemes, one pulse can only create one modulation (or echo) of substantial amplitude. However, if the tipping angles are larger than 1°, e.g., 3°, the echo shape will change due to the inclusion of other coherence pathways that produce overlapping signals [6]. These multiple coherence pathways exhibit different flow-induced phase shifts, thus complicating the echo shape and phase shift analysis. As a result, these previous methods are limited to very small tipping angles and consequently may use only a small fraction of the available magnetization and a significant fraction of the magnetization is still left along the z-axis. In contrast, the MMME sequences can

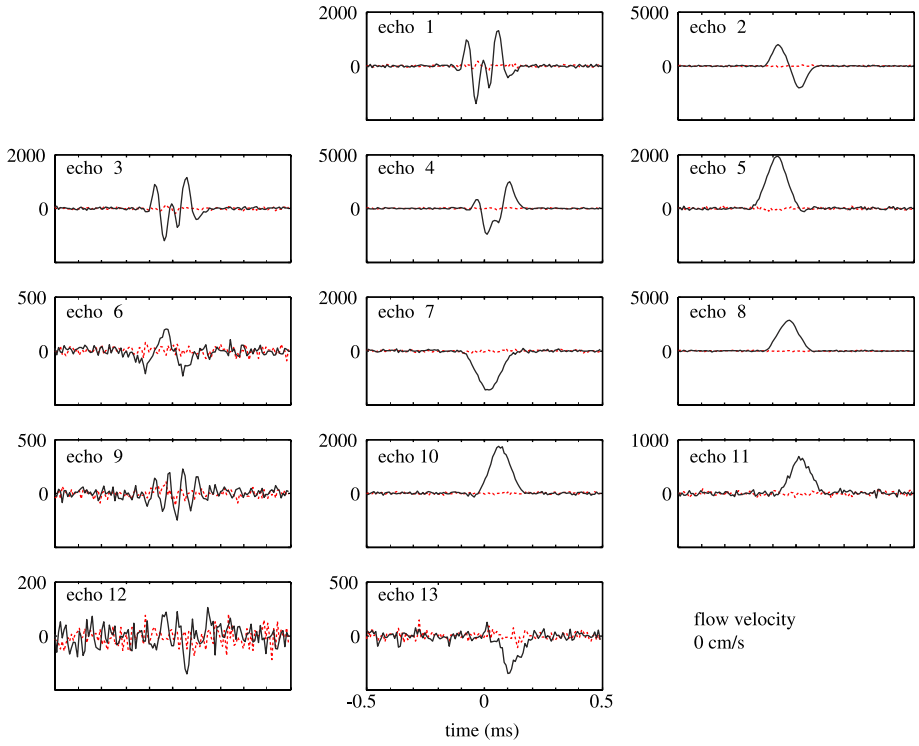

Fig. 1. Experimental echo shapes of MMME4 obtained on a stationary sample with $\tau_1/\tau_2/\tau_3 = 1/3/9$ ms. The dashed and solid lines are for real and imaginary parts, respectively, and the echo number is listed. The horizontal axis is the detection time and the time zero is defined by Eq. (10). The sample is a 5-mm NMR tube filled with distilled water. The field gradient is 10 G/cm along the tube axis. A phase correction of 50° was applied to the raw data so that the real part of the signal is essentially zero.

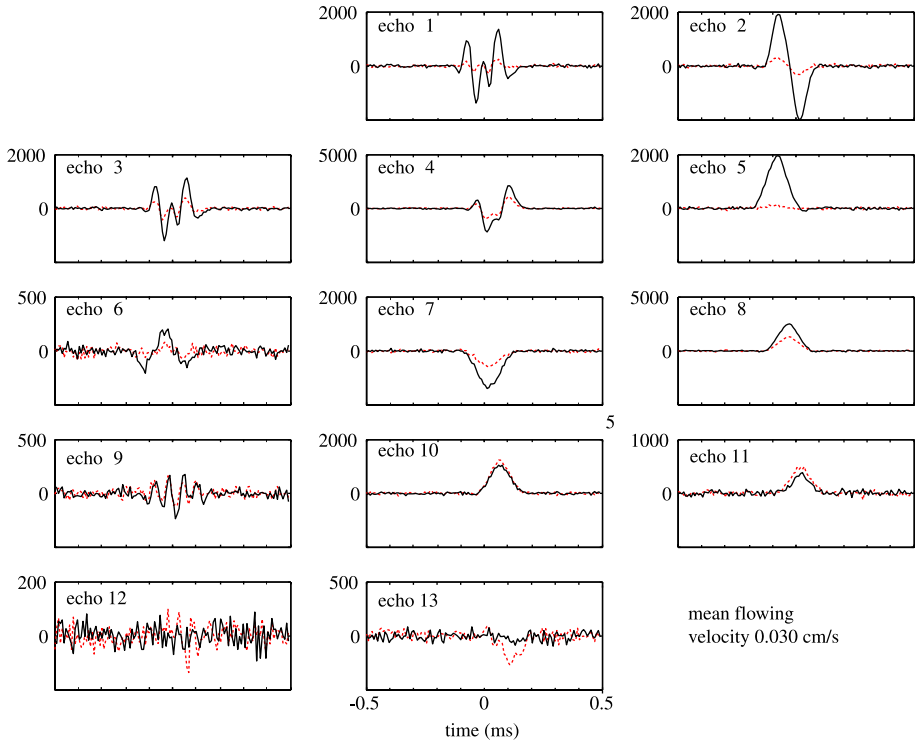

Fig. 2. Experimental echo shapes of MMME4 obtained on a flowing sample with $\tau_1/\tau_2/\tau_3 = 1/3/9$ ms. The dashed and solid lines are for real and imaginary parts, respectively, and the echo number is listed. The horizontal axis is the detection time and the time zero is defined by Eq. (10). The sample is a 5-mm NMR tube filled with distilled water. The field gradient is 10 G/cm along the flowing direction. A phase correction of 50° was applied to the raw data to illustrate the different phases of the echoes as compared to Fig. 1.

utilize essentially all of the magnetization. A detailed comparison of MMME with previous one-scan methods for diffusion has been discussed in [6].

3. Results

The sample used in the experiments was a 5-mm NMR tube connected to a flow system that is capable of constant volume flow velocity. The inner diameter of the NMR tube is 0.424 cm. The mean flow velocity used was ranging from 0.01 to 35 cm/s. The NMR experiments were carried out in a horizontal bore 2 T magnet (Nalorac Cryogenics) with a Bruker console (Bruker Biospin). The MMME4 sequence was used with $\tau_1/\tau_2/\tau_3 = 1/3/9$ ms for most of the flow rates except the fastest ones. The lengths of the four RF pulses are 40/40/40/80 μs, equivalent to nominal flip angles of 45/45/45/90°. The phases of the RF pulses are all zero.

We have obtained experimentally all 13 echoes of MMME4 shown in Fig. 1 for a stationary sample. These data serve as the reference for our experiments under flow conditions. A constant phase of 50° was applied to the raw signals to rotate the signal into the imaginary channel, with negligible signal in the real channel. The signals are consistent with the results of [6]. The shapes of the echoes are very different from each other. Each echo corresponds to a different coherence pathway, and the excitation spectrum is determined primarily by the off-resonance effects of the RF pulses for each coherence pathway. For example, echo 7 originates from $Q = (0, 1, -1, 1, -1)$, a coherence pathway that is similar to a Hahn echo where each of last three RF pulses inverts the magnetization. The resulting echo shape is therefore similar to that of a Hahn echo. For other echoes, the excitation spectra can be modulated in the frequency domain. Note that the maximum amplitude of the echoes does not always occur at the time zero defined by Eq. (10) due to the modulated excitation spectra. The details of the excitation spectra and the echo shapes of MMME has been discussed in [6] and can be calculated theoretically using the formalism developed in [4–6].

The 13 echoes are shown in Fig. 2 for the sample with a constant mean flow velocity of 0.030 cm/s. The same 50° phase correction used for the stationary reference measurement was applied again. Now the echo shapes show a non-zero real part in many echoes, indicating the phase shifts of the signals. For example, the real part of the signals is comparable with the imaginary part for echo 8–11. For numerical data processing, we define the signal phase ϕ_1 for the ith echo $f_i(t)$ by minimizing the real part of $f_i(t)\exp(-i\phi_1)$. This phase factor ϕ_1 is determined for the MMME echoes at a series of flow velocities and some of the results are shown in Fig. 3. For fast flow, we have used a reduced field gradient and τ's to measure mean flow velocities up to 35 cm/s.

In Fig. 3A, the phase shift is shown as a function of c_Q for three flow velocities. c_Q is evaluated using Eq. (7). For each flow velocity, the phase shift is shown to be proportional to c_Q, consistent with Eq. (5). The proportionality coefficient obtained from the plot for each flow rate agrees with in a few percent with the mean flow velocity calculated from the volume flow rate. Please note that the 13 data points for each flow rate were obtained in one scan. The signal-to-noise ratio for some of the echoes can be improved by an optimal choice of the tipping angles of the RF pulses [6].

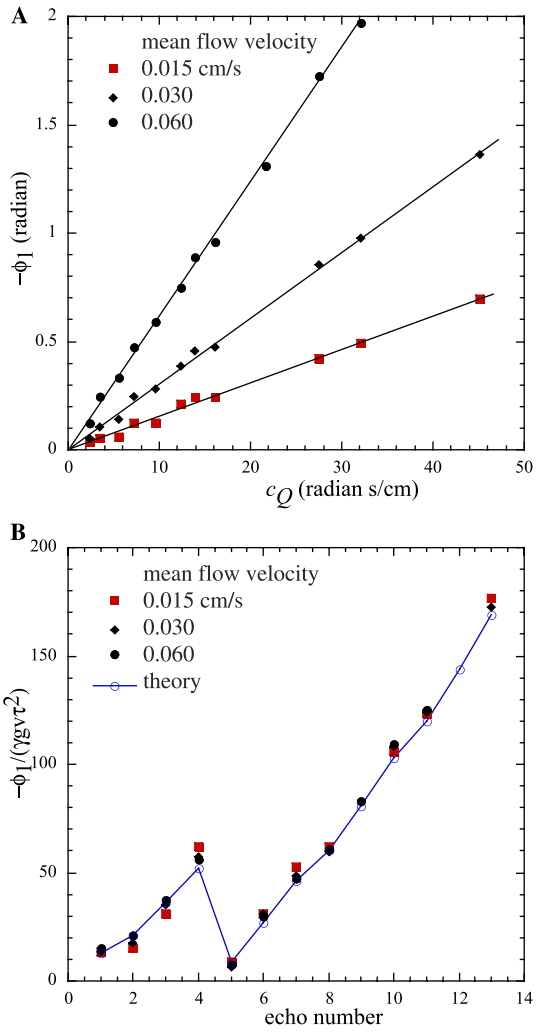

Fig. 3. Plots of flow-induced phase shift at three flow rates of mean flow velocities (v): 0.060, 0.030, and 0.015 cm/s. The MMME4 experiments were performed with the $\tau_1/\tau_2/\tau_3 = 1/3/9$ ms. A field gradient was along the flow direction, $g = 10$ G/cm. (A) A plot of ϕ_1 as a function of c_Q calculated using Eq. (7). The data points for each flow rate fall on the straight line and the slope of the lines is found to agree with the mean flow velocities, respectively. The lines are linear fit to the data. (B) A plot of $\phi_1/(\gamma g v \tau^2)$ for all echoes at the three flow rates. The open circles are from theoretical evaluation of $c_Q/\gamma g \tau^2$, using Eq. (7) and they are consistent with the experimental results.

For an MMME experiment with a constant gradient, one may derive from Eq. (7) that $c_Q/(\gamma g\tau^2)$ is a unitless constant that depends only on the coherence pathways (i.e., echo number) and the ratio of the τ_i periods. The experimental results ($\phi_1/\gamma v g\tau^2$) for the three flow rates are shown in Fig. 3B and are found to be in good agreement with the theoretical evaluation of $c_Q/(\gamma g\tau^2)$ for all echoes.

For fluid flow in a pipe, the distribution of the fluid velocity and displacement often is broad. One can easily integrate Eq. (3) over the velocity distribution and find that a distribution of velocities results in a non-zero ϕ_1 and a reduction in the echo amplitude. When the phase shift is small, $\phi_1 \ll 1$, ϕ_1 will always measure the mean velocity. In Poiseuille pipe flow the distribution of velocities and displacements is symmetric about the mean velocity, and the flow-induced phase shift (ϕ_1) will be proportional to the c_Q-value associated with the coherence pathway of each echo. It is worth noting that when the distribution of velocities and displacements is not symmetric about the mean value [10,11], the phase of the echoes may no longer be exactly linear in c_Q. Higher order cumulants of the displacement distribution can then in principle be inferred from the phase of the signal. If sufficiently many suitable values of c_Q's can be probed, the velocity distribution can be obtained by this a single-shot method.

4. Conclusions

We present an NMR method for a truly rapid measurement of movement and flow. Because all coherence pathways are separated in the time domain, there is no need of repetitive scans for phase cycling, and it is thus a true one-scan method. We outline the theoretical framework to understand the complex echo shapes and flow sensitivity and found excellent agreement with experiments. Although a pulsed field gradient was not used in this paper, it is compatible with the current methodology.

One of the applications of this technique may be the observation of time-sensitive processes such as in fluid characterization, medical MRI, and the monitoring of material processing and chemical reactions.

Acknowledgments

We thank M. Hürlimann and D. Madio for discussions and comments.

References

[1] E.L. Hahn, Spin echoes, Phys. Rev. 80 (1950) 580.
[2] E.O. Stejskal, J.E. Tanner, Spin diffusion measurements: spin echoes in the presence of a time-dependent field gradient, J. Chem. Phys. 42 (1965) 288.
[3] P.T. Callaghan, Principles of nuclear magnetic resonance microscopy, Oxford University Press, New York, 1993.
[4] M.D. Hürlimann, Diffusion and relaxation effects in general stray field NMR experiments, J. Magn. Reson. 148 (2001) 367.
[5] Y.-Q. Song, Categories of coherence pathways in the CPMG sequence, J. Magn. Reson. 157 (2002) 82.
[6] Y.-Q. Song, X. Tang, A one-shot method for measurement of diffusion, J. Magn. Reson. 170 (2004) 136.
[7] S.J. Doran, M. Décorps, A robust, single-shot method for measuring diffusion coefficients using the "Burst" sequence, J. Magn. Reson. A 117 (1995) 311.
[8] S. Peled, C.H. Tseng, A.A. Sodickson, R.W. Mair, R.L. Walsworth, D.G. Cory, Single-shot diffusion measurement in laser-polarized gas, J. Magn. Reson. 140 (1999) 320.
[9] I.J. Lowe, R.E. Wysong, DANTE ultrafast imaging sequence (DUFIS), J. Magn. Reson. B 101 (1993) 106.
[10] U.M. Scheven, P.N. Sen, Spatial and temporal coarse graining for dispersion in randomly packed spheres, Phys. Rev. Lett. 89 (25) (2002) 254501.
[11] R. Kubo, M. Toda, N. Hashitsume, Statistical Physics II, Springer-Verlag, New York, 1991.